Available online at www.sciencedirect.com
ScienceDirect
Journal of the European Ceramic Society 29 (2009) 2325–2332
www.elsevier.com/locate/jeurceramsoc

Dielectric and piezoelectric properties of Cu^{2+}-doped alkali Niobates

N. Marandian Hagh [a], K. Kerman [a], B. Jadidian [b], A. Safari [a,*]

[a] Department of Materials Science and Engineering, Rutgers University, The State University of New Jersey, 607 Taylor Road, Piscataway, NJ 08854, USA
[b] J&W Medical LLC, 56 Partrick Rd., Westport, CT 06880, USA

Received 25 September 2008; received in revised form 12 December 2008; accepted 8 January 2009
Available online 20 February 2009

Abstract

The effect of Cu^{2+} addition (0.5–2 mol%) on microstructure and electromechanical properties of lead-free piezoelectric system of $(K_{0.44}Na_{0.52}Li_{0.04})(Ta_{0.1}Sb_{0.06}Nb_{0.84})O_3$ (KNN-LT-LS) was investigated through two processing methods; namely perovskite and mixed-oxide. The addition of Cu^{2+} showed an increase in grain size and relative density of the undoped ceramics in both processing techniques. Introduction of Cu^{2+} stabilized the orthorhombic phase at room temperature by shifting the tetragonal–orthorhomic phase transition to higher temperatures while did not show any major changes in T_c. The polarization-field response of Cu^{2+}-doped ceramics showed a decline in both remnant polarization and coercive field, thus reducing the area of the hysteresis loop. This shrinkage in hysteresis loop was manifested through a large improvement in mechanical quality factor, nearly 4 times that of undoped ceramic. Within the studied range of Cu^{2+} addition, the ceramic with 0.5 mol% of Cu^{2+} prepared by mixed-oxide route represented a relatively desirable balance between the degradation of the electromechanical properties, improvement in temperature stability, and mechanical quality factor.

Keywords: Lead-free piezoelectrics; Dielectric properties; Niobates; Perovskites; Piezoelectric properties

1. Introduction

Lead-free piezoelectric materials were utilized in applications prior to the introduction of lead zirconate titanate [PZT or $Pb(Zr_{1-x},Ti_x)O_3$] in the 1950s in Japan.[1] Lead based materials are more widely used as piezoelectric materials in transducer devices due to their superior electromechanical properties.[2] Despite this, the high lead content in their compositions has raised environmental and safety concerns regarding proper handling, disposal and recycling.[3,4] Legislation on electrical and electronic equipment waste and restriction of hazardous substances (RoHS) has been recently enforced as the directive in the European Union[5–8] which may highly impact piezoelectric manufactures in future. In fact, this global action has sparked enough momentum for scientists to search for lead-free alternative materials with comparable dielectric and electromechanical properties to their lead-based counterparts.

Among different lead-free compositions, potassium sodium niobate ($K_{0.5}Na_{0.5}NbO_3$; KNN) solid solutions have shown promising electromechanical properties comparable with lead-based piezoceramics.[9] The potassium sodium niobate (KNN) composition is composed of equi-molar solid solution of $KNbO_3$ (KN) and $NaNbO_3$ (NN).[1,10,11] Both KN and NN demonstrate orthorhombic symmetry at room temperature. Although the former shows ferroelectric behavior, the latter demonstrates an anti-ferroelectric response.[12] Pioneering works on the binary and ternary compositions of KNN–$LiTaO_3$ and KNN–$LiTaO_3$–$LiSbO_3$ reported by Saito et al., have explicitly shown that the piezoelectric properties comparable to MPB of PZT, as well as barium and lanthanum doped PZT, can indeed be achieved.[9,13–15] The piezoelectric charge coefficient of the binary system falls in the range of 150–230 pC/N and the ternary system shows a d_{33} = 300 pC/N, with their Curie temperatures of being in 170–500 and 253 °C, respectively. The substitution of the Sb^{5+} and Ta^{5+} in octahedral sites of NbO_6 in the ternary system of KNN-LT-LS gives rise to a "soft" ferroelectric behavior, which improves the piezoelectric and coupling coefficients while increasing dielectric loss and reducing the mechanical quality factor.

* Corresponding author.
E-mail address: safari@rci.rutgers.edu (A. Safari).

0955-2219/$ – see front matter © 2009 Elsevier Ltd. All rights reserved.
doi:10.1016/j.jeurceramsoc.2009.01.003

The improved electromechanical properties of KNN-LT-LS ceramics make them suitable candidate as soft lead-free ferroelectric materials for actuators, sensors, low[16] and high frequency[17] ultrasonic transducer devices. However, the usage of this ternary system is undesirable for high power transducer applications, due to the instability of its coupling coefficients with small temperature variations, its high dielectric loss ($\tan\delta$: 1.7–4%) and low mechanical quality factor (Q_m: 50–85). Introducing additives is an effective way of minimizing the temperature sensitivity, reducing the dielectric loss, and enhancing mechanical quality factor. Previous researchers have shown that the addition of Cu^{2+} to alkali niobate systems results in an improvement in sinterability, microstructure texturing and mechanical quality factor.[18–21]

The objective of the present study was to demonstrate the effect of Cu^{2+} addition on the microstructure, phase transition, crystal structure, and electromechanical properties of $(K_{0.44}Na_{0.52}Li_{0.04})(Ta_{0.1}Sb_{0.06}Nb_{0.84})O_3$ system in order to be used as a "hard" ferroelectric material for high power ultrasonic transducers.

2. Experimental procedure

The compositions of interest were synthesized by two processing routes of perovskite and mixed-oxide according to the chemical formula of $(K_{0.44}Na_{0.52}Li_{0.04})(Ta_{0.1}Sb_{0.06}Nb_{0.84})O_3 + x\text{CuO}$, where x is the mole fraction of the Cu^{2+} dopant (x = 0.0, 0.5, 1.0, 1.5, 2.0). The details of powder processing and synthesis are described in Ref. 22. The prepared powders were uni-axially pressed and sintered at 1150 °C for 1 h in an oxygen atmosphere (O_2 flow rate of 360 cm^3/min). The top and bottom surfaces of the pellets were polished down to about 0.5 mm and Au electrode was deposited by DC sputtering. The samples were poled under an electric field of 30 kV/cm for 15 min in a silicon oil bath at 100 °C.

The microstructures of the sintered samples were studied by field emission scanning electron microscopy (FESEM) LEO (ZEISS) 982. Grain size measurements were carried out using the mean intercept length method from different areas of the sample. Qualitative X-ray phase analysis was carried out on X-ray diffractometer Philips D500 with Cu K_α radiation using a step-scan of 0.03°/step in 2θ and 1 s dwell time/step. Piezoelectric charge coefficient, d_{33}, was directly recorded from a Berlincourt piezometer (Channel Products, Inc.) by averaging ten readings from each surface of the ceramic pellets. Poisson's ratio was measured from the ratio of the first overtone to the fundamental resonance frequency ($f_s^{(2)}/f_s$) of the planar mode in accordance to the IEEE standards.[23] Piezoelectric planar, thickness and the 31 mode coupling coefficients, (k_p, k_t, and k_{31}) were calculated from the resonance and anti-resonance frequencies of the impedance traces, based on the IEEE standard. Longitudinal coupling coefficient, k_{33}, was estimated from the thickness and planar coupling coefficients.[1] Planar and thickness frequency constants were obtained from resonance frequencies of planar f_s^p and thickness f_s^t modes, respectively. Using an HP 4194A impedance/gain-phase analyzer, the planar mechanical quality factor was calculated using[23]:

$$Q_m = \frac{1}{R}\sqrt{\frac{L}{C_a}} \qquad (1)$$

where the R, L, and C_a are the resistance, inductance and capacitance in the equivalent electrical circuit of the piezoelectric resonator, respectively.

3. Results and discussion

3.1. Sintering and microstructural analysis

The addition of Cu^{2+} changed the average grain size and grain morphology in both perovskite and mixed-oxide routes as depicted in Fig. 1. Average grain size in undoped ceramics was 2.5 and 3 μm for perovskite and mixed-oxide routes, respectively. Addition of 2 mol% Cu^{2+} increased the average grain size to about 4 μm in perovskite and 5 μm in mixed-oxide routes. Densities of ceramics were also slightly increased and reached 97.6% and 97.3% for perovskite and mixed-oxide routes, respectively. In addition, grain morphology changed from sharp-cornered cubical grains with smooth surfaces to cut-cornered grains with rough surfaces. It appeared that introducing the Cu^{2+} altered the growth behavior of the grains by decreasing the surface energy. Based on the Jackson solid–liquid interface model, high entropy of fusion ($\Delta S_f > 2R$; R: 1.9872 cal/mol K) thermodynamically favors the layer by layer growth and, therefore, creates atomically smooth growth surface.[24] However, at lower entropy of fusion ($\Delta S_f < 2R$), there is no preferential growth and hence random growth with rough surfaces occurs. It was hypothesized that the addition of Cu^{2+} decreased the entropy of fusion in KNN-LT-LS system by lowering its surface free energy, thus giving rise to the observed rough surfaces.

3.2. Phase analysis

Fig. 2 shows X-ray diffraction patterns of the sintered KNN-LT-LS ceramics with different molar percentages of Cu^{2+} prepared by mixed-oxide route (X-ray patterns of both routes were quite similar, thus only the mixed-oxide route was selected and discussed here). As shown, the solid solution of Cu^{2+} in KNN-LT-LS structure was observed with no detectable second phase within the dopant range of 0–2 mol%. Li et al.[20] reported the presence of second phase $K_4CuNb_8O_{23}$ in the Cu^{2+} added $(K_{0.44}Na_{0.52}Li_{0.04})(Ta_{0.1}Sb_{0.04}Nb_{0.86})O_3$ ceramic when the Cu^{2+} addition exceeded from 0.1 mol%. The disparity in results could be attributed to the slight compositional difference (higher Sb^{5+}/Nb^{5+} ratio in current study than Li's), different powder precursors, and processing procedure.

The X-ray diffraction pattern of the base composition (0% Cu^{2+}) showed the coexistence of two structures namely orthorhombic and tetragonal phases at room temperature. Introducing Cu^{2+} in the range of $0 < x \leq 1.0$ mol% stabilized the orthorhombic structure. Further increase in concentration of Cu^{2+} beyond 1.0 mol% reduced the splitting of (2 2 0) and

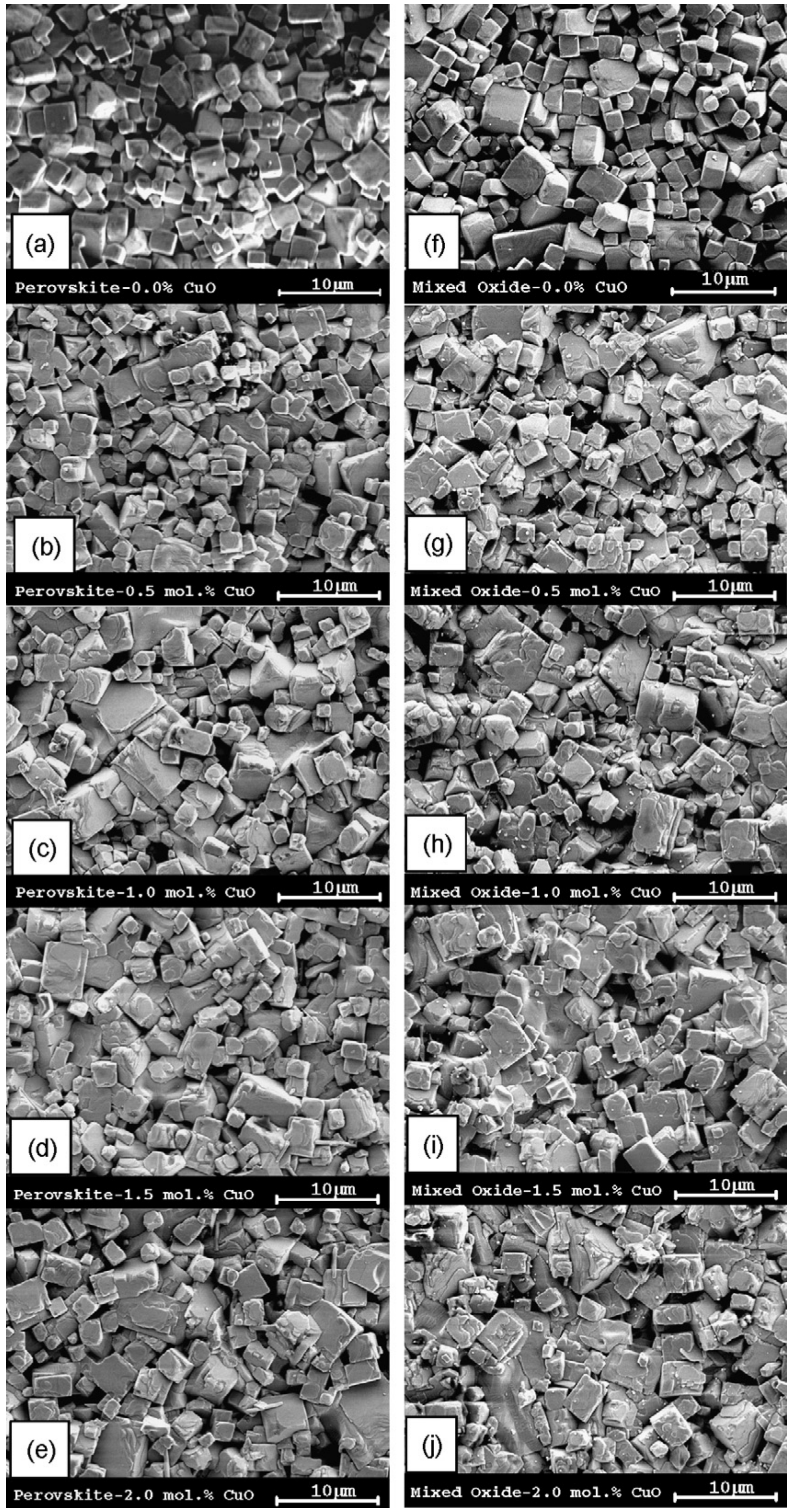

Fig. 1. SEM microstructure of the 0, 0.5, 1, 1.5, and 2 mol% Cu-doped KNN-LT-LS ceramics prepared through (a–e) "perovskite" and (f–j) "mixed-oxide" routes.

(0 0 2) orthorhombic reflections. This implied that the dopant was still incorporated into the perovskite structure in the form of solid solution even at doping level of 2 mol%. At 1.5 and 2 mol% Cu^{2+} concentrations, merging of (2 2 0) and (0 0 2) was observed, seemingly pointing to a phase transition to tetragonal. While it did not match with tetragonal structure, the X-ray pattern suggested that the transition leaned favorably toward distorted orthorhombic. This observation was also confirmed by permittivity–temperature measurements which will be discussed in Section 3.3.

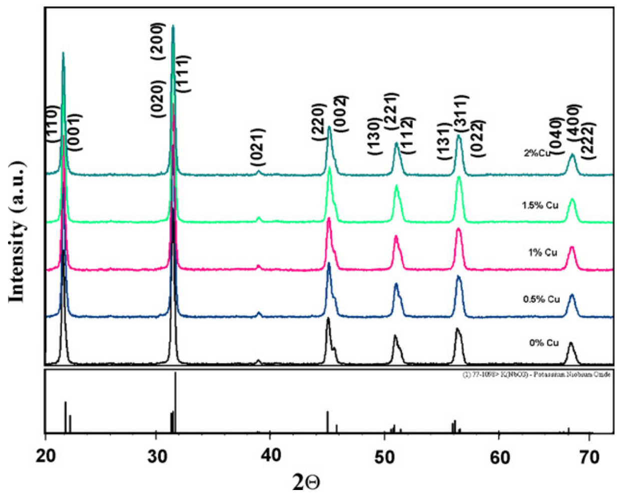

Fig. 2. X-ray diffraction patterns of the 0, 0.5, 1, 1.5, and 2 mol% Cu^{2+}-doped KNN-LT-LS ceramics prepared by "mixed-oxide route".

3.3. Temperature dependence of relative permittivity and dielectric loss

Temperature dependence of relative permittivity and dielectric loss were measured upon cooling at the frequency of 1 kHz in the temperature range of 0–380 °C. As illustrated in Fig. 3a and b, both perovskite and mixed-oxide routes showed similar temperature–permittivity behaviors with three distinctive regions separated by two phase transitions. For undoped ceramics, the orthorhombic–tetragonal ($T_{o–t}$) and tetragonal–cubic (Curie temperature; T_c) phase transitions occurred at ∼34 and 264 °C, respectively. Relative permittivity peaks at T_c were sharp and had the highest value for undoped ceramic. Addition of the Cu^{2+} gave rise to a sharp decrease in K_{max} without affecting the Curie temperature. This is in good agreement with the results reported for Cu^{2+}-doped alkali niobate systems on lowering permittivity especially at the Curie point. Saito and Takao[18] and Lin et al.[21] reported the insensitivity of Curie temperature to the introduction of 0.01 and 1 mol% Cu^{2+} to KNN. However, Li et al. observed a slight change in T_c (∼4 °C upon 0.3 wt% Cu^{2+}).[20]

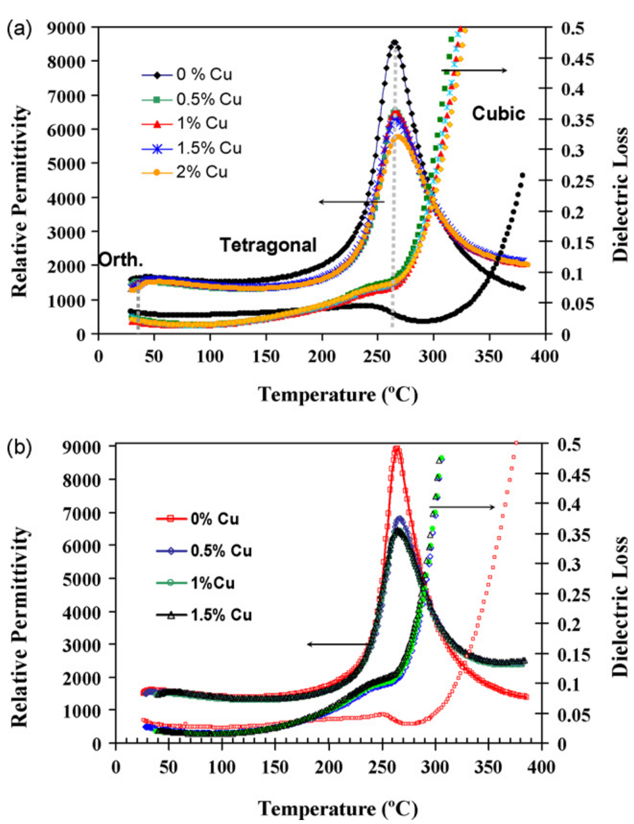

Fig. 3. Temperature dependence of relative permittivity and dielectric loss, upon Cu^{2+} addition on KNN-LT-LS ceramics prepared by (a) "perovskite" and (b) "mixed-oxide" route. Measured frequency: 1 kHz.

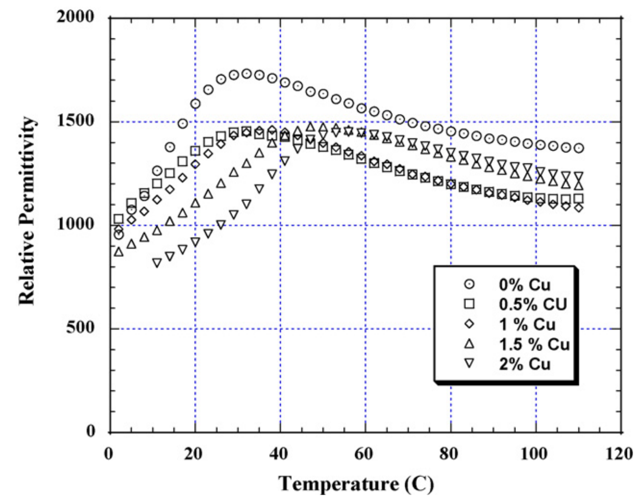

Fig. 4. Temperature dependence of permittivity for Cu^{2+}-doped KNN-LT-LS ceramics prepared by mixed-oxide route and measured at 1 kHz.

Despite the insensitivity of the T_c to the addition of Cu^{2+}, the room temperature phase transition temperature (orthorhombic–tetragonal; $T_{o–t}$) shifted toward higher temperature upon addition of Cu^{2+} in both processing techniques (Fig. 4). The increase in room temperature transition point ($T_{o–t}$) was up to 22 and 24 °C for both pervoskite and mixed-oxide routes, respectively. Introducing higher Cu^{2+} (1.5 and 2 mol%) contents to the structure of the KNN-LT-LS resulted in diffuse phase transition shown by wider permittivity peak. Temperature dependence of dielectric loss showed the similar trend of changes in both processing methods. At temperatures <175 °C, the Cu^{2+}-doped ceramics had lower dielectric loss compared to the undoped ceramic. While at the temperatures >175 °C and particularly above T_c, the addition of Cu^{2+} resulted in a sharp increase in dielectric loss values and shifting the loss patterns toward room temperature. This was mainly due to a decrease in bulk resistivity of KNN-LT-LS ceramics at higher temperatures, where the ceramic becomes electrically conductive.

3.4. Electromechanical properties

Room temperature dielectric properties of Cu^{2+}-doped KNN-LT-LS ceramics are shown in Fig. 5a and e. Addition of Cu^{2+} up to 0.5 mol% to the base compositions, drastically decreased both relative permittivity and dielectric loss (33% and 67%, respectively; in perovskite route). Further addition

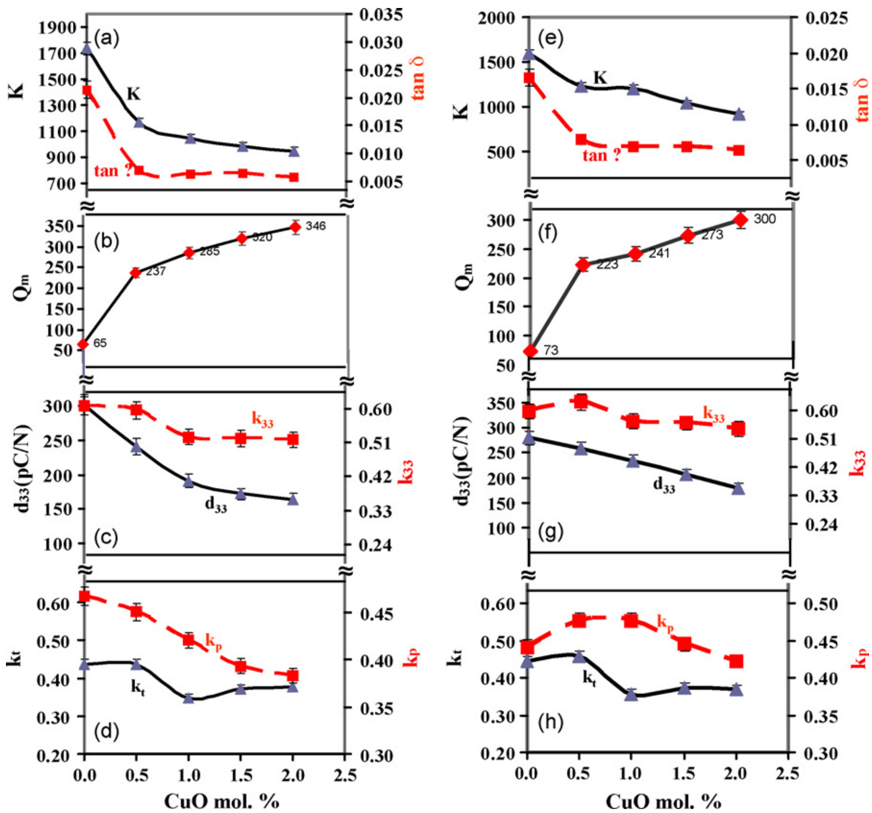

Fig. 5. Effect of Cu^{2+} addition on dielectric and piezoelectric properties of Cu^{2+}-doped KNN-LT-LS ceramics prepared through (a–d) "perovskite" and (e–h) "mixed-oxide" routes.

of Cu^{2+} (>0.5 mol%) resulted in a gradual decline of relative permittivity.

The sharp decline of dielectric loss was accompanied by an abrupt rise in mechanical quality factor. The mechanical quality factor measured at minimum impedance $|Z_m|$ of the fundamental resonance is generally defined as the ratio of in-phase strain to out-of-phase strain with stress, and analogous to electrical quality factor, is inversely related to dielectric loss or dissipation factor. Since the extent of the mechanical Q is determined by the presence of the movable domain walls, the energy loss from the domain wall motions suppresses the mechanical vibration of the resonator. This mechanical damping which is converted into heat lowers the Q_m value and increases the dissipation factor. It appears that the addition of Cu^{2+} has reduced the energy loss of the KNN-LT-LS system by restricting the domain wall motions and causing less interference with mechanical vibration of the ceramic resonator. The high Q_m is desirable especially for high power ultrasonic applications, where the energy loss and generated heat are critical factors affecting the performance of transducer.

The relationship between mechanical Q and dielectric loss can be clearly seen from the sharp incline in Q_m values due to the drastic decrease in dissipation factor. As illustrated in Fig. 5b and f, notable improvement (three times more than those of undoped ceramics) in mechanical quality factor was achieved at 0.5 mol% Cu^{2+}. At higher concentrations of additive (>0.5 mol%), the rate of increase was not that significant and approached a linear type of variation (from 0.5 to 2 mol%). Meanwhile, improvement in mechanical quality factor was the highest at 2 mol% additive (about five times that of undoped ceramic). Fig. 5c and g depicts piezoelectric charge and coupling coefficients of Cu^{2+}-doped KNN-LT-LS ceramics. The addition of Cu^{2+} lowered both piezoelectric charge and longitudinal coupling coefficients. In addition, introduction of the additive had a pronounced effect on reducing the d_{33}. The decrease in piezoelectric charge coefficient could be due to the "hardening" effect, which lowers the piezoelectric charge and coupling coefficients, as well as the dielectric loss. It is believed that the decline in piezoelectric properties upon Cu^{2+} addition was due to the stabilization of orthorhombic phase at room temperature. This would consequently contribute to a smaller number of possible polarization directions. The effect of Cu^{2+} addition on thickness and planar coupling coefficients are shown in Fig. 5d and h.

3.5. Polarization-field response in doped KNN-LT-LS

Fig. 6a and b illustrates the room temperature field dependence of polarization for Cu^{2+}-doped KNN-LT-LS ceramics measured at 50 Hz. The incorporation of Cu^{2+} lowered the hysteresis loop with regards to undoped ceramic. The hysteresis loop in polarization-field response of a piezoelectric resonator represents the energy required to switch the meta-stable dipole moments during the short application of E-field. The larger the area of hysteresis loop, the higher the energy required to reverse dipoles. In fact, the area of hysteresis shows the amount of dissipated energy in the form of heat. Addition of Cu^{2+} lowered the

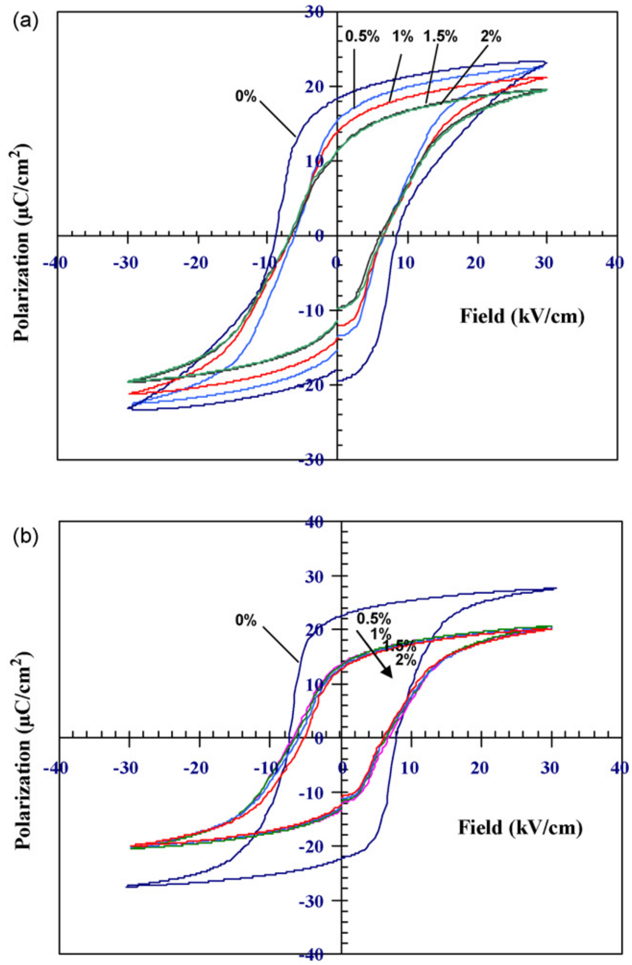

Fig. 6. Polarization-field response of the Cu^{2+}-doped KNN-LT-LS ceramics prepared from (a) perovskite and (b) mixed-oxide routes.

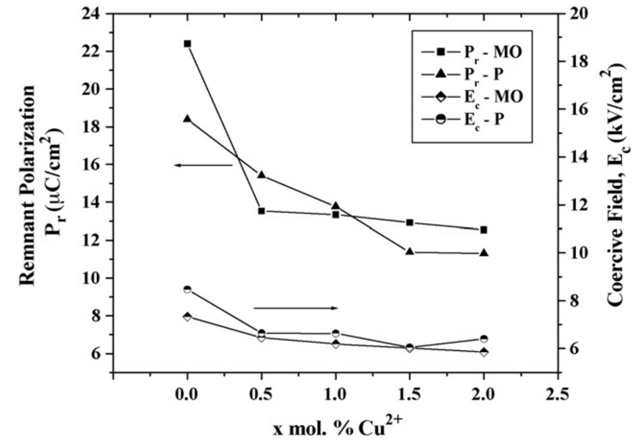

Fig. 7. Effect of Cu^{2+} addition on remnant polarization P_r and coercive field E_c of KNN-LT-LS ceramics prepared through "mixed-oxide" and "perovskite" routes. MO: mixed-oxide and P: perovskite.

hysteresis area, and therefore the amount of dissipated energy. The effect of Cu^{2+} addition on dissipation factor (dielectric loss) was already shown in Fig. 5a and e. It appeared that the results of polarization-field were in good agreement with the dielectric loss measurements. This implied that the 0.5 mol% Cu^{2+} was the most effective dopant concentration, as it facilitated the domain wall switching and led to the lower dissipation factor.

Fig. 7 summarizes the effect of Cu^{2+}on the polarization and coercive field of KNN-LT-LS ceramics. As shown, the coercive fields for both processing techniques comparatively decreased at similar rates. Typical hard ferroelectrics are known for their relatively low dielectric loss, high mechanical Q and high coercive field which are obtained by B-site acceptor substitution. Substitution of the lower valence cation in higher valence B-site induces the oxygen vacancies in the microstructure. These oxygen vacancies reduce the volume of the cell and are believed to play a major role in the 'hardening" effect.[1] In the current Cu^{2+}-doped system, the ionic radius of Cu^{2+} with coordination number of 6 ($r_{Cu^{2+}}$: 0.87 Å) falls in the size range of A-site (r_{K^+} : 1.52 Å , r_{Na^+} : 1.16 Å , r_{Li^+} : 0.90 Å) and B-site ($r_{Nb^{5+}}$: 0.64 Å , $r_{Ta^{5+}}$: 0.64 Å , $r_{Sb^{5+}}$: 0.60 Å) positions.[20] Based on ionic size, pauling's rules and the fact that perovskite structures have a relatively compact structure with less possibility of interstitial site occupancy, the Cu^{2+} ion could substitute in either A- or B-site locations. By considering these two possibilities one can write the Kroeger–Vink's notation[25] for each process of Cu^{2+} substitution in A and B sites as:

$$\mathrm{CuO} \rightarrow \mathrm{Cu}_{\mathrm{A}}^{\circ} + \mathrm{O}_o + V_{\mathrm{A}}' \quad (2)$$

$$2\mathrm{CuO} \rightarrow 2\mathrm{Cu}_{\mathrm{B}}''' + 2\mathrm{O}_o + 3V_o^{\circ\circ} \quad (3)$$

In A-site substitution (Eq. (2)), Cu^{2+} replaces the K^+, Na^+, or Li^+ cations (designated by A) which induces the A-site vacancy in the structure. This reaction process might be favorable due to the high volatility of the Li^+, K^+, and Na^+ especially above 1000 °C.[26–28] The B-site substitution (Eq. (3)) which Cu^{2+} replaces the Nb^{5+}, Ta^{5+}, or Sb^{5+} cations in octahedral sites, gives rise to substantial numbers of vacant sites in anion array, 3 oxygen vacancies for two Cu^{2+} cation substitutions. As it was discussed earlier in this section, this large number of oxygen vacancies was assumed to be responsible for "hardening" effect of the Cu^{2+}-doped KNN-LT-LS ceramic. However, it was expected that this would consequently increase the coercive

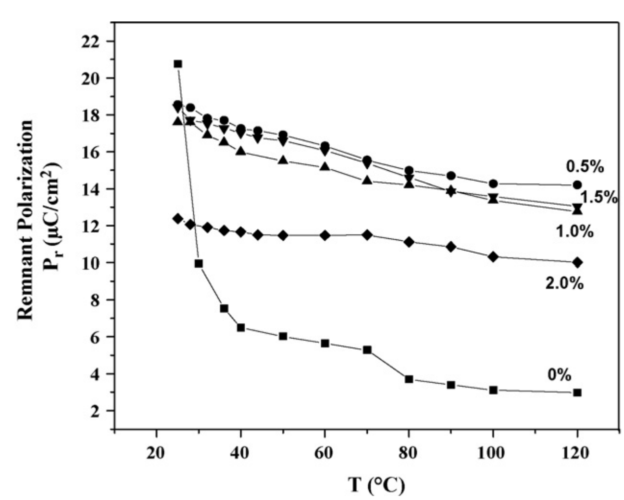

Fig. 8. Temperature dependence of polarization for Cu^{2+}-doped KNN-LT-LS ceramics obtained through mixed-oxide process.

Table 1
Dielectric and electromechanical properties of Cu^{2+} (0.5 mol%) doped KNN-LT-LS prepared by perovskite and mixed-oxide routes.

Material	$\varepsilon_{33}^T/\varepsilon_o$	$\tan\delta$ (%)	d_{33} (pC/N)	k_p	k_t	k_{33}	k_{31}	Q_m	N_p (Hz.m)	N_t (Hz.m)	P_r (μC/cm^2)	E_c (kV/cm)
Perovskite (0.5% Cu^{2+})	1170	0.7	240	0.45	0.44	0.60	0.26	240	3360	3035	15.4	6.7
Mixed-oxide (0.5% Cu^{2+})	1230	0.8	260	0.48	0.46	0.63	0.27	225	3290	2980	13.5	6.9

field of the doped ceramic. In contrast, the decrease of coercive field and the improvement of Q_m implied that Cu^{2+} could be substituted in both A- and B-sites.

3.6. Temperature dependence of polarization

In order to study the temperature stability of Cu^{2+}-doped ceramics, the temperature dependence of remnant polarization was measured within the temperature range of 20–120 °C. As shown in Fig. 8 the undoped ceramics showed higher remnant polarizations at room temperature. In the case of Cu^{2+}-doped ceramics, despite the lower initial remnant polarization at room temperature, they demonstrated a relatively stable polarization. As illustrated in Fig. 8, the polarization retention (%) at 120 °C relative to those at room temperature for all Cu^{2+}-doped ceramics was above 70%, while this value for undoped ceramic was only 15%. It was anticipated that the improved polarization stability upon Cu^{2+}-doping was directly related to the stabilization of orthorhombic phase at room temperature and the hardening effect of Cu^{2+} in KNN-LT-LS microstructure. The improved polarization stability could also be due to the substitution of Cu^{2+} especially in B-site which largely affected the domain wall stabilization through the oxygen vacancy increase and manifested in the form of improved Q_m.

4. Summary and conclusions

The effect of copper (0.5–2 mol%) on microstructure, phase transition and electromechanical properties of $(K_{0.44}Na_{0.52}Li_{0.04})(Nb_{0.84}Ta_{0.1}Sb_{0.06})O_3$ system was studied through the perovskite and mixed-oxide routes. Introduction of Cu^{2+} to KNN-LT-LS structure increased the grain size and changed the growth behavior of the grains. Addition of Cu^{2+} also modified the morphology of grains from sharp-cornered cubical grains with smooth surface to cut-cornered grains with rough surfaces. It was anticipated that the addition of Cu^{2+} lowered the entropy of fusion for KNN-LT-LS system through a decline in its surface free energy. Relative density of Cu^{2+}-doped ceramics were slightly increased with dopant concentration and reached to about more than 97% (at 2 mol% Cu^{2+}) for both preparation techniques.

Phase analysis of Cu^{2+}-doped KNN-LT-LS ceramics showed solid solubility up to 2 mol% with no detectable second phase. Addition of Cu^{2+} ($0 > x \geq 1.0$) stabilized the orthorhombic phase at room temperature. While at higher doping concentrations the merging of (2 2 0) and (0 0 2) peaks represented the possibility of distorted orthorhombic phase. The addition of Cu^{2+} did not change the tetragonal–cubic phase transition (Curie temperature, T_c); however, it shifted the orthorhombic–tetragonal phase transition to higher temperatures.

Addition of Cu^{2+} drastically lowered the room temperature dielectric loss ($\tan\delta$) and significantly improved mechanical quality factor (Q_m). Piezoelectric charge and coupling coefficients (planar k_p, thickness k_t and longitudinal k_{33}) were slightly degraded upon doping. This is mainly due to the stabilization of the orthorhombic phase at room temperature and the fact that the undoped ceramics benefited from larger number of polaization directions. Field dependence of polarization showed that polarizability level and coercive field for Cu^{2+}-doped KNN-LT-LS ceramics decreased. As summarized in Table 1, mixed-oxide route with relatively high piezoelectric charge, d_{33}: 260 pC/N (∼13% lower than undoped ceramic) and longitudinal coupling coefficients of k_{33}: 0.63, provided large improvement in Q_m (∼4 times), drastic decrease in dielectric loss (>50%), and more than 70% retention of remnant polarization at 120 °C. The results of this study suggest that the lead-free Cu^{2+}-doped KNN-LT-LS ceramic might be a good candidate for high power ultrasonic transducer applications.

Acknowledgement

The financial support of Glenn Howatt foundation at the electroceramic laboratory of Rutgers University is acknowledged.

References

1. Jaffe, B., *Piezoelectric Ceramics*. Academic Press, New York, 1971, pp. 214–217.
2. Tressler, J. F., Alkoy, S. and Newnham, R. E., Piezoelectric sensors and sensor materials. *J. Electroceram.*, 1998, **2**(4), 257–272.
3. Li, Y., Moon, K.-S. and Moon, C. P., Electronics without lead. *Science*, 2005, **308**, 1419–1420.
4. United States Environmental Protection Agency, *Health and Environmental Impacts of Lead*, http://www.epa.gov/air/lead, 2008 [last updated on 10.15.08].
5. European Union, *Restriction of Hazardous Substances* (*RoHS*), Directive 2002/95/EC. http://eurlex.europa.eu/LexUriServ/LexUriServ.do?uri=OJ:L:2003:037:0019:0023:EN:Pdf.
6. Demartin Maeder, M., Bamjanovic, D. and Setter, N., Lead-free piezoelectric materials. *J. Electroceram.*, 2004(13), 385–392.
7. Pecht, M., Fukuda, Y. and Rajagopal, S., The impact of lead-free legislation exemptions on the electronic industry. *IEEE Trans. Electron. Packaging Manuf.*, 2004, **27**(4), 221–232.
8. Directive 2008/34/EC of the European Parliament and of the Council, Amending directive 2002/96/EC on Waste Electrical and Electronic Equipment (WEEE). *Official Journal of the European Union*, 2008 (March). Available on line at: http://eur-lex.europa.eu/en/index.htm.
9. Saito, Y., Takao, H., Tani, T., Nanoyama, T., Takatori, K., Homma, T. *et al.*, Lead-free piezoceramics. *Nature*, 2004, **123**, 84–87.
10. Shirane, G., Newnham, R. and Pepinsky, R., Dielectric properties and phase transitions of $NaNbO_3$ and (Na, K)NbO_3. *Phys. Rev.*, 1954, **96**, 581–588.
11. Egerton, L. and Dillon, D. M., Piezoelectric and dielectric properties of the ceramics in the system potassium–sodium niobate. *J. Am. Ceram. Soc.*, 1959, **42**, 438–442.

12. Cross, L. E., Electric double hysteresis in $(K_xNa_{1-x})NbO_3$ single crystals. *Nature*, 1958, **181**, 178–179.
13. Guo, Y., Kakimoto, K. and Ohasto, H., $(K_{0.5}Na_{0.5})NbO_3$–$LiTaO_3$ lead-free piezoelectric ceramics. *Mater. Lett.*, 2005, **59**, 241–244.
14. Saito, Y. and Takao, H., Nb-Perovskite Structured Piezoelectric Ceramics for Sensors and Actuators. In *The twelfth US–Japan seminar on dielectric and piezoelectric ceramics*, 2005.
15. Nonoyama, T., Nagaya, T., Saito, Y., Takatori, K., Homma, T. and Takao, H., Piezoelectric ceramic compostion, its production method, and piezoelectric device and dielectric device. US Patent #0178605A1, 2003.
16. Marandian Hagh, N., Ashbahian, E., Jadidian, B. and Safari, A., Lead-free piezoelectric ceramic transducer in the donor-doped $K_{1/2}Na_{1/2}NbO_3$ solid solution system. *IEEE Trans. Ultrason. Frequency Control*, 2008, **55**(1), 214–224.
17. Jadidian, B., Marandian Hagh, N., Winder, A. and Safari, A., 25 MHz ultrasonic transducers with lead-free piezoceramic, 1-3 PZT fiber-epoxy composite, and PVDF polymer active elements. *IEEE T. Ultrason. Ferr.*, 2009, **56**(2), 368–378.
18. Saito, Y. and Takao, H., Nb-perovskite structured piezoelectric ceramics for sensor and actuator. In *The 12th US–Japan seminar on dielectric and piezoelectric ceramics*, 2005, pp. 103–107.
19. Takao, H., Saito, Y., Aoki, Y. and Horibuchi, K., Microstructural evolution of crystalline-oriented $(K_{0.5}Na_{0.5})NbO_3$ piezoelectric ceramics with a sintering aid of CuO. *J. Am. Ceram. Soc.*, 2006, **89**(6), 1951–1956.
20. Li, E., Kakemoto, H., Wada, S. and Tsurumi, T., Influence of CuO on the structure and piezoelectric properties of the alkaline niobate-based lead-free ceramics. *J. Am. Ceram. Soc.*, 2007, **90**(6), 1787–1791.
21. Lin, D., Kwok, K. W. and Chan, H. L. W., Double hysteresis loop in Cu-doped $K_{0.5}Na_{0.5}NbO_3$ lead-free piezoelectric ceramics. *Appl. Phys. Lett.*, 2007, **90**, 232903.
22. Marandian Hagh, N., Jadidian, B. and Safari, A., Property-processing relationship in lead-free (K, Na, Li) NbO_3-solid solution system. *J. Electroceram.*, 2007, **18**(3–4).
23. The Institute of Electrical and Electronics Engineers (IEEE), *Standards on Piezoelectricity*. American National Standards Institute, 1987, ANSI/IEEE Std. 176.
24. Martin, E. and Glicksman, *Diffusion in Solids: Field Theory, Solid-State Principles and Applications*. John Wiley Inter-science Publishers, New York, NY, 1999.
25. Kroeger, F. A., *Chemistry of Imperfect Crystals*. North-Holland, Amesterdam, Netherlands, 1964.
26. Kakimoto, K.-I., Masuda, I. and Ohsato, H., Lead-free $KNbO_3$ piezoelectric ceramics synthesized by pressure-less sintering. *J. Eur. Ceram. Soc.*, 2005, **25**, 2719–2722.
27. Kim, M., Lee, D.-S., Park, E.-C., Jeong, S.-J. and Song, J.-S., Effect of Na_2O additions on the sinterability and piezoelectric properties of lead-free $95(Na_{0.5}K_{0.5})NbO_3$–$5LiTaO_3$ ceramics. *J. Eur. Ceram. Soc.*, 2007, **27**, 4121–4124.
28. Bomlai, P., Wichianrat, P., Muensit, S. and Milne, S., Effect of calcination conditions and excess alkali carbonate on the phase formation and particle morphology of $Na_{0.5}K_{0.5}NbO_3$ Powders. *J. Am. Ceram. Soc.*, 2007, **90**(5), 1650–1655.